Journal of Statistical Mechanics: Theory and Experiment
An IOP and SISSA journal

PAPER: Interdisciplinary statistical mechanics

Statistical characterization of the standard map

Guiomar Ruiz[1,2], **Ugur Tirnakli**[2,3], **Ernesto P Borges**[4,5] **and Constantino Tsallis**[2,5,6,7]

[1] Departamento de Matemática Aplicada y Estadística, Universidad Politécnica de Madrid, Pza. Cardenal Cisneros s/n, 28040 Madrid, Spain
[2] Centro Brasileiro de Pesquisas Fisicas Rua Xavier Sigaud 150, Rio de Janeiro 22290-180, Brazil
[3] Department of Physics, Faculty of Science, Ege University, 35100 Izmir, Turkey
[4] Instituto de Física, Universidade Federal da Bahia, Salvador-BA 40170-115 Brazil
[5] National Institute of Science and Technology for Complex Systems Rua Xavier Sigaud 150, Rio de Janeiro 22290-180, Brazil
[6] Santa Fe Institute, 1399 Hyde Park Road, Santa Fe, New Mexico 87501, United States of America
[7] Complexity Science Hub Vienna, Josefstädter Straße 39, 1080 Vienna, Austria
E-mail: guiomar.ruiz@upm.es, ugur.tirnakli@ege.edu.tr, ernesto@ufba.br and tsallis@cbpf.br

Received 17 April 2017
Accepted for publication 11 May 2017
Published 15 June 2017

Online at stacks.iop.org/JSTAT/2017/063403
https://doi.org/10.1088/1742-5468/aa728b

Abstract. The standard map, paradigmatic conservative system in the $(x,\ p)$ phase space, has been recently shown (Tirnakli and Borges (2016 *Sci. Rep.* **6** 23644)) to exhibit interesting statistical behaviors directly related to the value of the standard map external parameter K. A comprehensive statistical numerical description is achieved in the present paper. More precisely, for large values of K (e.g. $K=10$) where the Lyapunov exponents are neatly positive over virtually the entire phase space consistently with Boltzmann–Gibbs (BG) statistics, we verify that the q-generalized indices related to the entropy production q_{ent}, the sensitivity to initial conditions q_{sen}, the distribution of a time-averaged (over successive iterations) phase-space coordinate q_{stat}, and the relaxation to the equilibrium final state q_{rel}, collapse onto a fixed point, i.e. $q_{\text{ent}}=q_{\text{sen}}=q_{\text{stat}}=q_{\text{rel}}=1$. In remarkable contrast, for small values of K (e.g. $K=0.2$) where the Lyapunov exponents are virtually zero over the entire phase space, we verify $q_{\text{ent}}=q_{\text{sen}}=0$, $q_{\text{stat}}\simeq 1.935$, and $q_{\text{rel}}\simeq 1.4$. The situation

1742-5468/17/063403+14$33.00

corresponding to intermediate values of K, where both stable orbits and a chaotic sea are present, is discussed as well. The present results transparently illustrate when BG behavior and/or q-statistical behavior are observed.

Keywords: nonlinear dynamics

Contents

1. Introduction 2
2. Sensitivity to initial conditions 3
3. The rate of entropy production 4
4. The rate of relaxation of the entropy 8
5. Stationary distributions 9
6. Concluding remarks 12
Acknowledgments 13
References 13

1. Introduction

Statistical characterization of dynamical systems, particularly weakly chaotic low-dimensional dissipative maps, have been made according to its sensitivity to the initial conditions, the rate of increase of the entropy, the rate of relaxation to the attractor, and the distribution of a statistical variable [1]. For strongly chaotic systems, these behaviors present an exponential nature and are described by the Boltzmann–Gibbs (BG) statistical mechanical framework [2]. On the other hand, weakly chaotic systems, that present zero *largest Lyapunov exponent* (LLE) λ, need a more general formalism to be conveniently handled. It has been observed that the nonextensive statistical mechanical framework is able to describe different features of various classes of complex systems [3–18]. If the LLE approaches zero, the sensitivity to the initial conditions and the rate of relaxation to the attractor follow q-exponential behaviors, the distributions exhibit a q-Gaussian form, and the rate of increase of entropy demands S_q entropy. All these behaviors are parameterized by the indices q_{sen}, q_{ent}, q_{rel}, q_{stat}, for *sensitivity*, *entropy production*, *relaxation*, and *stationary distribution*, respectively. It has been observed (and in some instances proved) that, for low-dimensional systems, $q_{\text{sen}} = q_{\text{ent}}$, through the q-generalized Pesin identity [1]. Consequently, three (possibly related) quantities remain to be addressed, that are currently referred to as the q-triplet [1]. The q-triplet has been experimentally observed in a variety of complex systems like in the ozone layer [19] and in the Voyager I data for the solar wind [20], among many others. The possible relations between the q-triplet indices should in principle exhibit the fixed point $q = 1$ in BG statistical regimes. This happens whenever the LLE is positive. In fact, the LLE plays a central role in the determination of which statistical framework is to be used in the description of nonlinear dynamical systems.

In the present work we address a low-dimensional conservative system, namely the standard map [21, 22]:

$$p_{i+1} = p_i - K \sin x_i \qquad ; \qquad x_{i+1} = x_i + p_{i+1} \tag{1}$$

where p and x are taken as modulo 2π. Its phase space can exhibit strongly (weakly) chaotic regions characterized by positive (zero) local LLE. The LLE has been numerically evaluated through the Benettin *et al* algorithm [23] for each initial condition separately [24, 25]. For sufficiently small values of K, for instance $K = 0.2$, virtually the entire phase space exhibits stable orbits (zero LLE), and if K takes high values ($K = 10$), the points of the phase space have finite positive values of LLE. In the present work, we numerically evaluate the values of $q_{\rm sen}$, $q_{\rm ent}$, and $q_{\rm rel}$ for both strongly and weakly chaotic cases. We also revisit the stationary distributions that have been recently found in [24], and particularly the mixed case, where both strongly and weakly chaotic regions exist. Finally, we exhibit the interplay, within the stationary distributions, between strongly and weakly chaotic $q_{\rm stat}$ indices for arbitrary values of K.

J. Stat. Mech. (2017) 063403

2. Sensitivity to initial conditions

The sensitivity to initial conditions is given by

$$\xi(t) = \lim_{\|\boldsymbol{\Delta} x(0)\| \to \mathbf{0}} \frac{\|\boldsymbol{\Delta} x(t)\|}{\|\boldsymbol{\Delta} x(0)\|}, \tag{2}$$

where $\boldsymbol{\Delta} x(t)$ is the temporal dependence of the discrepancy of two very close initial conditions at time t. When ergodic behavior dominates, equation (2) is expressed by the exponential dependence,

$$\xi(t) = \mathrm{e}^{\lambda t} \tag{3}$$

and λ is the standard LLE. Strongly chaotic systems are those which present $\lambda > 0$. Strong insensitivity to initial conditions corresponds to $\lambda < 0$. The marginal case $\lambda = 0$ is governed by a rule which is more subtle than equation (3) [26], namely:

$$\xi(t) = \exp_{q_{\rm sen}}(\lambda_{q_{\rm sen}} t), \tag{4}$$

where $\exp_q x \equiv [1 + (1-q)x]_+^{1/(1-q)}$ is the so called q-exponential function [27] with $[u]_+ = \max\{u, 0\}$ (with $\exp_1 x = e^x$), and $\lambda_{q_{\rm sen}}$ is a generalized Lyapunov coefficient. If $\lambda_{q_{\rm sen}} > 0$ the system is weakly chaotic, in the sense that $\xi(t)$ diverges slower than the exponential case, —asymptotically, a power law—. If the system is strongly chaotic, $q_{\rm sen} \to 1$, and equation (4) recovers the standard exponential dependence, with $\lambda_{q_{\rm sen}} \to \lambda_1 \equiv \lambda$.

The correctness of this description can be checked, for both regimes of standard map, in figure 1 (strongly chaotic regime) and figure 3 (weakly chaotic regime). They show, for different values of q, the averages of $\ln_q \xi(t)$ (where $\ln_q x \equiv (x^{1-q} - 1)/(1-q)$

is the inverse function of the q-exponential, and $\ln_1 x = \ln x$) over N_r realizations. Each realization starts with a randomly chosen pair of very close initial conditions, that are localized inside a particular cell of the W equally partitioned phase space. The case $W = 1$ represents averaging over N_r realizations, starting with randomly chosen pairs of initial conditions that are localized all over the whole phase space. We consider decreasing initial discrepancies in equation (2), so as to obtain a well defined behavior for increasingly long times (see figure 1(a)).

For the strongly chaotic case, exponential sensitivity to the initial conditions is verified with $q_{\text{sen}}^{\text{av}} = 1$, and the same generalized Lyapunov exponent characterizes the whole phase space, no matter the value of W (e.g. $W = 1$) or the particular cell inside of which the average is performed. In fact, the slope of all intermediate regimes in figure 1(b) exhibits $\lambda = \lambda_{q_{\text{sen}}^{\text{av}}=1} = 1.62$, in accordance with [29] (see also [30]).

For the weakly chaotic case, stability islands dominate the phase space. In this case, statistical characterization of the map was already tentatively done [31, 32]. But the characterization of cells evolution is much more intricate, and a common transient time can not be defined. This fact tends to preclude a neat linear dependence of $\langle \ln_{q_{\text{sen}}} \xi \rangle$ with time. Consequently, in weakly chaotic regimes, the N_r random pairs of initial conditions are not to be chosen all over the entire phase space but instead inside particular cells, so that their trajectories will go through cells with a similar spreading rate, and a transient time is susceptible to be simply defined (see figure 2). In this way, we verify that the map exhibits $q_{\text{sen}}^{\text{av}} = 0$, whose value of $\lambda_{q_{\text{sen}}^{\text{av}}}$ characterizes the local sensitivity to initial conditions, as it is shown in figure 3.

Summarizing, in both chaotic regimes we verify, after a transient, a nontrivial property [28] namely that there exists a special value of q, noted $q_{\text{sen}}^{\text{av}}$ (where av stands for *average* over the whole phase space for strongly chaotic regime), which yields a linear dependence of $\langle \ln_{q_{\text{sen}}^{\text{av}}} \xi \rangle$ with time. In other words, we verify $\langle \ln_{q_{\text{sen}}^{\text{av}}} \xi(t) \rangle \approx \lambda_{q_{\text{sen}}^{\text{av}}} t$.

3. The rate of entropy production

With respect to the entropy production per unit time, we may conveniently use the q-entropy ($k = 1$, henceforth) [1, 33]

$$S_q(t) \equiv k \frac{1 - \sum_{i=1}^{W} p_i^q}{q-1} = k \sum_{i=1}^{W} p_i \ln_q(1/p_i) \qquad \left[S_1 = S_{\text{BG}} \equiv k \sum_{i=1}^{W} p_i \ln(1/p_i)\right]. \tag{5}$$

The q-entropy production is estimated dividing the phase space in W equal cells, and randomly choosing $N_{\text{ic}} \gg W$ initial conditions inside one of the W cells (typically $N_{\text{ic}} = 10W$, so as to obtain statistically well defined results). We follow the spreading of points within the phase space, and calculate equation (5) from the set of occupancy probabilities $\{p_i(t)\}$ ($i = 1, 2, \ldots, W$). Fluctuations are of course present, but they can be reduced when we choose $N_c \gg 1$ initial cells within which the N_{ic} initial conditions are chosen, and average $S_q(t)$ over the N_c realizations. The proper value of the entropic parameter $q_{\text{ent}}^{\text{av}}$ is the special value of q which makes the averaged q-entropy production per unit time to be finite, which is ultimately related with the extensivity of the entropy. The q-entropy production per unit time is consequently obtained as

J. Stat. Mech. (2017) 063403

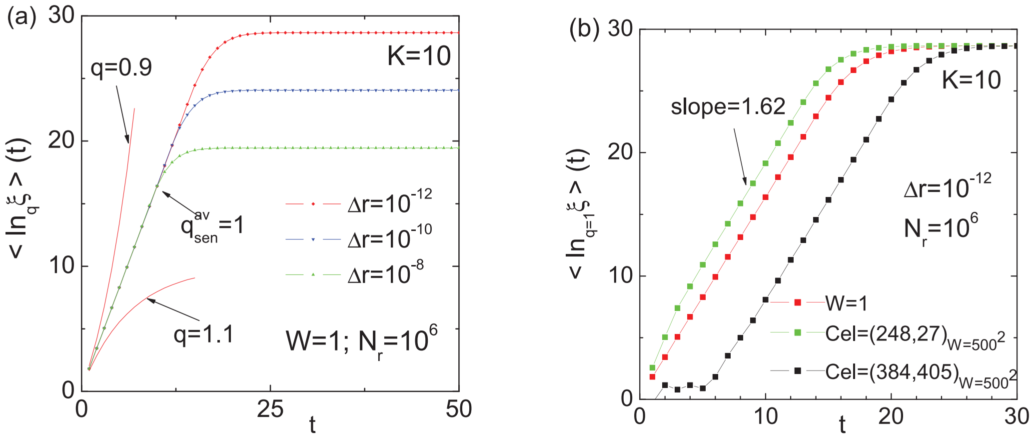

Figure 1. (a) Averages of $\ln \xi_q(t)$ over $N_r = 10^6$ realizations localized all over the whole phase space, i.e. $W = 1$ (see text), for $K = 10$. Decreasing Euclidean discrepancy of initial conditions $\Delta r \equiv \|\mathbf{\Delta} x(0)\|$ are considered, and $\langle \ln_{q_{\rm sen}^{\rm av}=1} \xi \rangle$ linear dependence with time is yielded in the $\Delta r \to 0$ limit. (b) Averages of $\ln \xi_q(t)$ over $N_r = 10^6$ realizations, for $K = 10$, and $\Delta r \equiv \|\mathbf{\Delta} x(0)\| = 10^{-12}$. The $N_r = 10^6$ pairs of initial conditions are randomly chosen over the whole phase space (red squares) and, amongst the $W = 500 \times 500$ cells of the equally partitioned phase, over one of the quickest spreading cells (green squares) and over one of the slowest spreading cells (black squares). In all cases, the slope is preserved in intermediate regimes.

$$K_{q_{\rm ent}^{\rm av}} = \lim_{t\to\infty} \lim_{W\to\infty} \lim_{N_{\rm ic}\to\infty} \frac{\langle S_{q_{\rm ent}^{\rm av}} \rangle_{N_c}(t)}{t} < \infty, \qquad (6)$$

and must be calculated taking into account that the partitions of phase space, N_c and $N_{\rm ic}$ are such as to obtain robust results.

When the LLE is large enough and the phase space is dominated by a chaotic sea, the BG entropy ($S_1 = S_{\rm BG} \equiv -\sum_{i=1}^{W} p_i \ln p_i$) is expected to be the appropriate one (i.e. $q_{\rm ent} = 1$). Fluctuations are reduced averaging over a set of $N_c = 0.01\,W$ randomly chosen initial cells localized all over the phase space. Our numerical results show, as expected, that the proper value of the entropic index is $q_{\rm ent}^{\rm av} = q_{\rm sen}^{\rm av} = 1$ for $K = 10$ (see figure 4). Both indices have been obtained comparing the nonlinearity measure of the polynomial fitting curves over the intermediate regime (after a transient and before saturation) were the correlation coefficient is constant and equals 1. Another interesting result that emerged is the coincidence of the slopes of the sensitivity and entropy functions of time (see figures 1 and 4), i.e. the q-entropy production per unit time satisfies $K_{q_{\rm sen}^{\rm av}=1} = \lambda_{q_{\rm sen}^{\rm av}=1}$. These results are numerically compatible with a q-generalized Pesin-like identity for ensemble averages in strongly chaotic conservative maps, and reinforce those in [28].

Entropic characterization of weakly chaotic regime in conservative maps is much more subtle [34, 35]. The phase space of weakly chaotic conservative maps exhibits stability islands and contains regions with a huge diversity of transient times. This framework makes a hard task to reduce fluctuations of $S_q(t)$ by averaging over N_c cells, and a convenient averaging criterion must be adopted.

The first practical difficulty that we find to discriminate N_c proper cells, in order to estimate $K_{q_{\rm ent}^{\rm av}}$ through equation (6), is the slow convergence of the finite time LLE to its

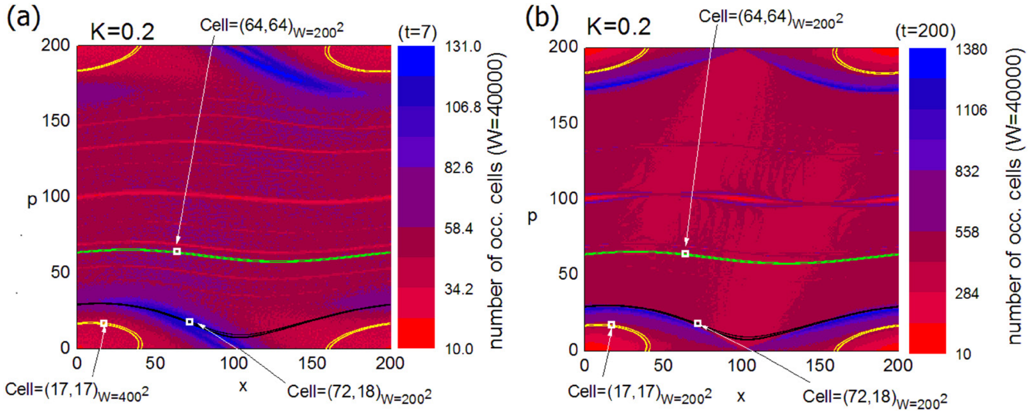

Figure 2. Color maps of the integrated number of occupied cells by the iteration 1 to the iteration t ($t = 7$ (a), $t = 200$ (b)) of 4×10^5 random initial conditions localized in the $(x\text{th}, p\text{th})$ cell of a $W = 200 \times 200$ equally partitioned phase space ($K = 0.2$). To warn about the different local transient times, we superimposed three particular cells and the trajectories of their respective interior initial conditions (yellow, black and green lines).

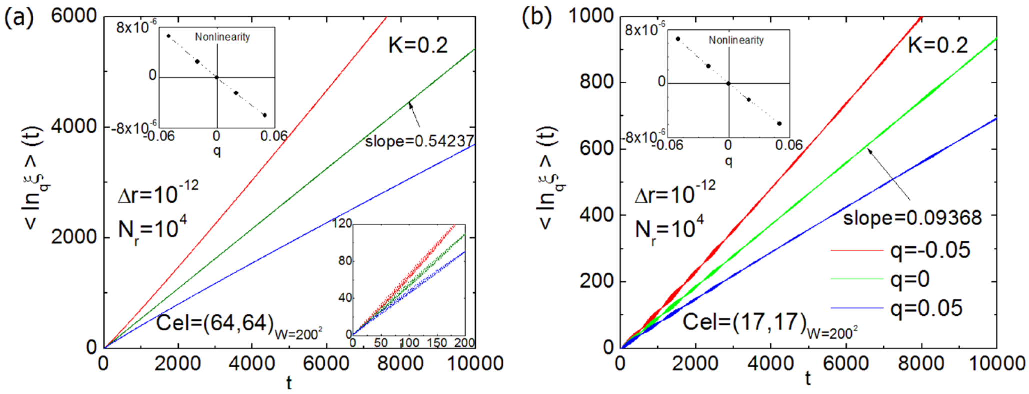

Figure 3. Averages of $\ln \xi_q(t)$ over $N_r = 10^4$ realizations whose initial conditions have been randomly chosen in (64th, 64th) (a), and (17th, 17th) (b) cells of the $W = 200 \times 200$ equally partitioned phase space of $K = 0.2$ standard map. A slightly oscillating evolution around q-exponential is observed for short times. Insets represent the nonlinearity measure $R \equiv C/B$ in the fitting curve of $\langle \ln \xi_q \rangle (t)$, $A + Bt + Ct^2$, and demonstrate that $q_{\text{sen}}^{\text{av}} = 0$ is the optimum value of q (a straight line fitting curve is obtained).

$t \to \infty$ limit value. Extremely long computer times are required, and it is for this reason that we tested the adequacy of the *smaller alignment index* (SALI) [36], instead of the LLE, to characterize weak chaos. First of all, we conclude that the SALI temporal evolution is a computationally cheap tool to characterize chaotic behavior of trajectories. In fact, the SALI tends to zero in both stable and chaotic orbits, but with completely different time rates: it decreases abruptly in strongly chaotic orbits and reaches the limit of accuracy of the computer after about 200 iterations. In contrast, it decreases with time as a power law in stable orbits. We have consequently verified, for the first time to the best of our knowledge, that the SALI decreases with time as a power law even in the case of weakly chaotic orbits. Besides, the power index of the *local* SALI

J. Stat. Mech. (2017) 063403

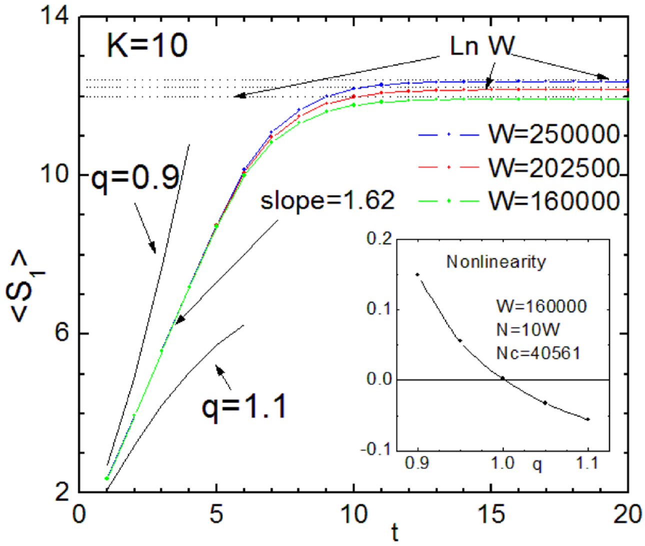

Figure 4. Temporal dependence of ($q_{\text{ent}}^{\text{av}} = 1$)-entropy in the standard map with $K = 10$, averaging over $N_c = 0.01\,W$ initial cells, for different values of the number of cells in the equally partitioned phase space, W. The case of $q < q_{\text{ent}}^{\text{av}} = 1$ ($q > q_{\text{ent}}^{\text{av}} = 1$) corresponds to positive (negative) concavity. The $t \to \infty$ limiting value is $\langle S_1 \rangle = \ln W$.

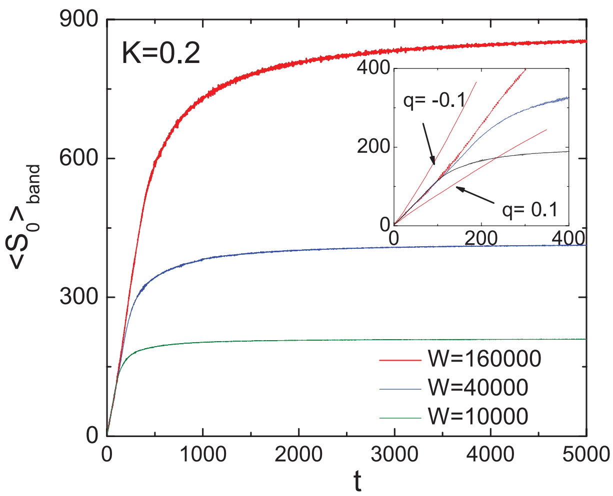

Figure 5. Increase of ($q_{\text{ent}}^{\text{av}} = 0$)-entropy in the standard map with $K = 0.2$, for different values of W, in a longitudinal band of phase space that covers $p = 2$, $x \in [0, 2\pi]$ (see text). The inset shows that $q < q_{\text{ent}} = 0$ ($q > q_{\text{ent}} = 0$) corresponds to positive (negative) concavity.

temporal evolution is also a computationally cheap resource to discriminate the initial cells that present similar transient entropy behavior. Identifying N_c cells that present a similar SALI temporal evolution, and obtaining the q-entropy production averaged over those N_c initial cells inside of which we randomly choose the N_{ic} initial conditions, $\langle S_q \rangle_{N_c}$ does not present the oscillations of entropy production typically observed in conservative maps [35]. Figure 5 exemplifies this fact, as $\langle S_q \rangle$ has been obtained averaging over a band of the phase space where the criterion of similar SALI evolution is fulfilled. Consequently, we confirm that a conservative system such as the standard map verifies the same statistical behavior than dissipative ones, i.e. there is a specific value of $q < 1$ in weak chaotic regime (for the logistic map, $q_{\rm ent} = 0.2445$ [30]) which yields finite entropy production per unit time, and hence $S_{q_{\rm ent}}$ is the proper entropy to thermodynamically characterize the system.

Summarizing, our numerical results show in both strongly and weakly chaotic regimes, as expected, $q_{\rm ent}^{\rm av} = q_{\rm sen}^{\rm av}$, which points towards the conjecture of the generalized Pesin equality [26]. In particular, $q_{\rm sen}^{\rm av} = q_{\rm ent}^{\rm av} = 1$ and $K_{q_{\rm ent}^{\rm av}} = \lambda_{q_{\rm sen}^{\rm av}} = 1.62$ for $K = 10$ (strong chaotic regime, since LLE >0), and $q_{\rm sen}^{\rm av} = q_{\rm ent}^{\rm av} = 0$ for $K = 0.2$ (weakly chaotic regime, since $\lambda \simeq 0$, $\lambda_{q_{\rm sen}^{\rm av}} > 0$).

We have also verified, for intermediate values of the parameter of the map that make the chaotic sea and the quasiperiodic trajectories coexist, that the regions of the phase space portrait where LLE $\neq 0$ verify $q_{\rm ent}^{\rm av} = q_{\rm sen}^{\rm av} = 1$ and $K_{q_{\rm ent}^{\rm av}} = \lambda_{q_{\rm sen}^{\rm av}}$, and the regions of the phase space portrait where LLE =0 verify $q_{\rm ent}^{\rm av} = q_{\rm sen}^{\rm av} = 0$ but quite frequently $K_{q_{\rm ent}^{\rm av}} \neq \lambda_{q_{\rm sen}^{\rm av}}$. In particular, we found $\lambda_{q_{\rm sen}^{\rm av}=1} = 0.47$ and $\lambda_{q_{\rm sen}^{\rm av}=1} = 0.88$, for the chaotic sea associated to the parameter values $K = 2$ and $K = 4$, respectively.

4. The rate of relaxation of the entropy

For the methods described in sections 2 and 3, we chose an ensemble of initial conditions inside one of the W cells of the phase space, and thus $S_q(0) = 0$, $\forall q$. Alternatively, an ensemble of initial conditions can be spread over the entire phase space of a *dissipative* system [37] and, therefore, the maximum possible value for the entropy is $S_{q_{\rm ent}}(0) = \ln_{q_{\rm ent}} W$. In that case, the time evolution brings the system to its attractor, and it has been observed that the number of occupied cells falls, and the entropy exponentially relaxes, in the case of a strongly chaotic system, or q-exponentially relaxes, in the case of a weakly chaotic system [38].

The method adopted in [37] cannot be identically applied to a conservative map, since there is no attractor, but the method introduced in [38] can be adapted to area-preserving models. We consider the variable $\Delta S_q(t) = S_q(\infty) - S_q(t)$ and evaluate its average over an ensemble of initial conditions for $t \to \infty$. The average must be computed with a different criterion in strongly and weakly chaotic regimes, according to their respective dynamical behavior in phase space.

The strongly chaotic map is dominated all over the partitioned phase space by a chaotic sea, and we can analytically calculate $S_{q=1}(\infty) = \ln W$. In that case, the average $\langle \Delta S_q(t) \rangle_{N_{\rm ic}}$ has been estimated over the most quickly spreading cells $N_{\rm ic}$, to minimize the computation time. On the contrary, the stability islands dominate the phase space in the weakly chaotic regime, and their respective value of $S_{q_{\rm ent}}(\infty) = \ln_{q_{\rm ent}} W_{\rm islands}$ (where $W_{\rm islands}$ is the number of occupied cells when the system achieves its stationary state) is unknown, as it numerically depends on the cells where the initial conditions are randomly chosen. Consequently, in weakly chaotic regimes, $S_{q_{\rm ent}}(\infty)$ must be first numerically estimated.

We verify, as expected, that $\lim_{W\to\infty} \Delta S_{q_{\rm ent}^{\rm av}} \sim \exp_{q_{\rm rel}^{\rm av}}(-t/\tau_q)$, where τ_q is a relaxation time. Figures 6(a) and (b) show the time dependence of $\ln_{q_{\rm rel}} \langle \Delta S_{q_{\rm ent}}(t) \rangle / \langle S_{q_{\rm ent}}(\infty) \rangle$ for

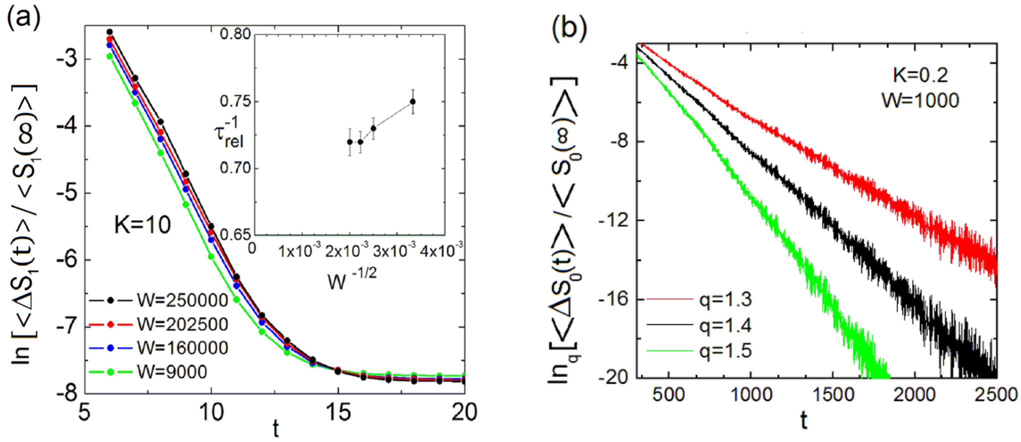

Figure 6. (a) Time evolution of $\ln_{q_{\rm rel}}\langle\Delta S_{q=1}(t)\rangle/\langle S_{q=1}(\infty)\rangle$ in the $K=10$ (strongly chaotic) standard map. The averages have been calculated over the more quickly spreading cells, to optimize the computational cost. Inset represents the numerical estimations of the inverse of relaxation time $\tau_{\rm rel}^{-1}(W^{-1/2})$. (b) Time evolution of $\ln_{q_{\rm rel}}\langle\Delta S_{q=0}(t)\rangle/\langle S_{q=0}(\infty)\rangle$ in the $K=0.2$ (weakly chaotic) standard map. The averages are calculated over the cells that belong to the same longitudinal band analyzed in figure 5. According to a procedure similar to what was done in figure 3, the nonlinearity measure identifies $q_{\rm rel}=1.4$.

the strongly chaotic case ($K=10$), and for the weakly chaotic case ($K=0.2$), respectively. The former case displays an exponential relaxation, i.e. $q_{\rm rel}=1$, consistently with BG framework. Observe that the numerical estimations of the inverse time of relaxation to the $S_{q_{\rm ent}=1}(\infty)$ entropy limit, are compatible with a finite relaxation time $\tau_{q=1}\equiv\tau_{\rm rel}(W\to\infty)$. The weakly chaotic case presents a q-exponential relaxation regime, with $q_{\rm rel}\simeq 1.4$ for $K=0.2$. The numerical estimation of $q_{\rm rel}$, for intermediate values of the map parameter K, is much more subtle because of the uncertainty related to the numerical estimation of $\ln_{q_{\rm ent}} W_{\rm islands}$.

5. Stationary distributions

Probability density distributions are among the most relevant items regarding the statistical description of nonlinear dynamical systems. Gaussian distributions are typical for ergodic and mixing systems, for which LLE is positive [24, 39], and q-Gaussian distributions are typical for weakly chaotic systems for which LLE$=0$ [24, 39–41].

We define the q-Gaussian distribution as

$$P_q(x;\mu_q,\sigma_q)=A_q\sqrt{B_q}\left[1-(1-q)B_q(x-\mu_q)^2\right]^{\frac{1}{1-q}}, \qquad (7)$$

where μ_q is the q-mean value, σ_q is the q-variance, A_q is the normalization factor and B_q is a parameter which characterizes the width of the distribution [42]:

$$A_q = \begin{cases} \frac{\Gamma\left[\frac{5-3q}{2(1-q)}\right]}{\Gamma\left[\frac{2-q}{1-q}\right]}\sqrt{\frac{1-q}{\pi}}, & q < 1 \\ \frac{1}{\sqrt{\pi}}, & q = 1 \\ \frac{\Gamma\left[\frac{1}{q-1}\right]}{\Gamma\left[\frac{3-q}{2(q-1)}\right]}\sqrt{\frac{q-1}{\pi}}, & 1 < q < 3 \end{cases} \tag{8}$$

$$B_q = [(3-q)\sigma_q^2]^{-1} \tag{9}$$

where $q \to 1$ recovers the Gaussian distribution $P_1(x;\mu_1,\sigma_1) = \frac{1}{\sigma_1\sqrt{2\pi}}\mathrm{e}^{-\frac{1}{2}\left(\frac{x-\mu_1}{\sigma_1}\right)^2}$.

Both Gaussian and q-Gaussian distributions have recently been observed for the standard map. In [24], the authors analyzed, for representative K values, the distribution of sums of iterates of the map

$$y = \sum_{i=1}^{T}(x_i - \langle x \rangle), \tag{10}$$

where $\langle \cdots \rangle$ represents both time average over T iterations and ensemble average over M initial conditions, i. e.

$$\langle x \rangle = \frac{1}{M}\frac{1}{T}\sum_{j=1}^{M}\sum_{i=1}^{T} x_i^{(j)}. \tag{11}$$

The probability distributions of y, namely $P(y)$, that emerge from the standard map with weakly chaotic phase space are q-Gaussians (say $q \equiv q_{\mathrm{stat}} \neq 1$), while Gaussian distributions are associated with the strongly chaotic regime (say $q \equiv q_{\mathrm{stat}} = 1$). The scenario for intermediate values of K is also quite rich. For these cases, the phase space displays regions with points that have positive LLE, —the chaotic sea—, and regions with $\lambda = 0$, —the stability islands. The probability distributions for initial conditions within the strongly chaotic regions are Gaussians ($q_{\mathrm{stat}} = 1$), and the probability distributions for initial conditions that belong to the weakly chaotic regions are q-Gaussians ($q_{\mathrm{stat}} \neq 1$). One remarkable feature is that, for initial conditions within weakly chaotic regions, $q_{\mathrm{stat}} \simeq 1.935$ in all cases, regardless the value of K.

Observe that if the initial conditions are spread over the entire phase space, the initial conditions are from both the chaotic sea and the stability islands. In that case, the distribution that emerges is a linear combination of a Gaussian and a q-Gaussian. Consequently, the probability distribution of the standard map, for any arbitrary value of K, can be modeled as

$$P(y) = \alpha P_q(y;\mu_q,\sigma_q) + (1-\alpha)P_1(y;\mu_1,\sigma_1). \tag{12}$$

where $P_q(y)$ and $P_1(y)$ are the probability densities for the initial conditions taken inside the weak and strong regions, respectively. In [24] it was taken the linear combination of the probability distributions normalized to the maximum value $P(0)$, and the physical meaning of the interpolating parameter was not clear.

Let us now take the linear combination of the usual probability densities in equation (12). First, we find out the ratio of the areas for the strongly and weakly chaotic regions. In order to achieve this, we randomly generate $N_{\mathrm{ic}} = 4 \times 10^6$ initial

J. Stat. Mech. (2017) 063403

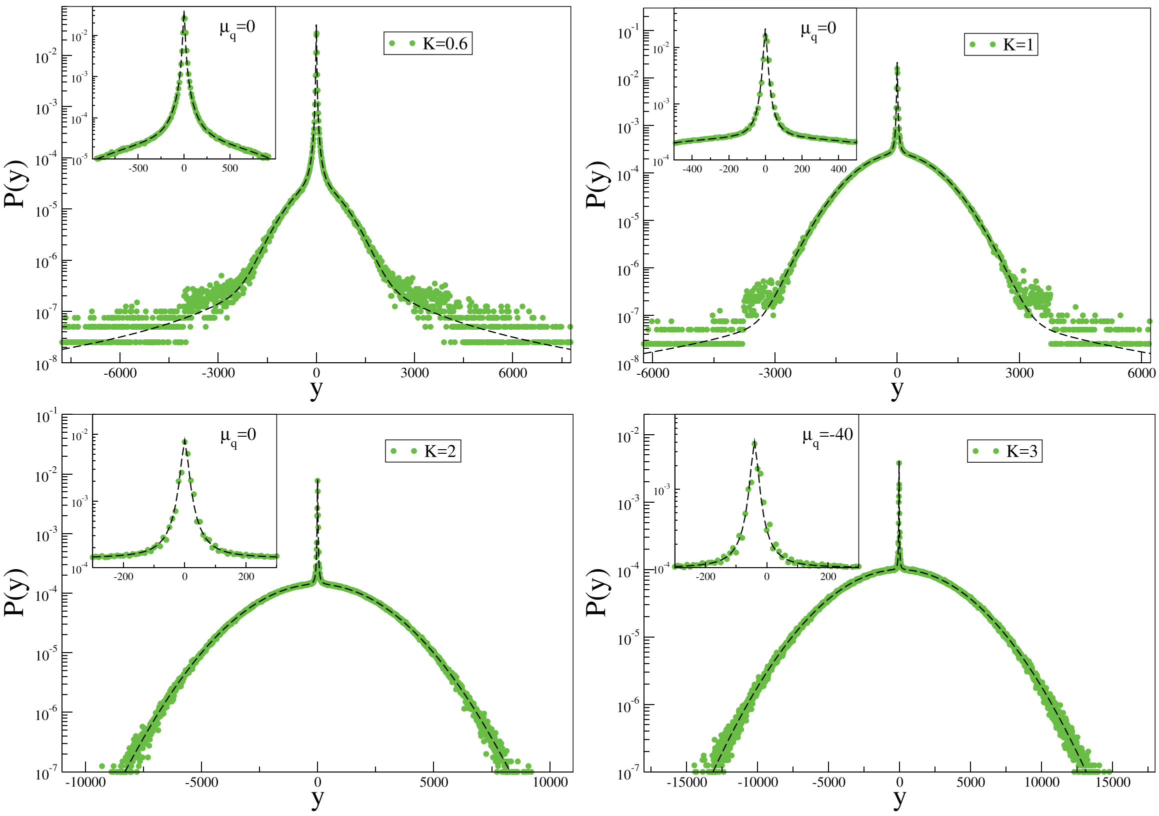

Figure 7. Probability distribution functions of the standard map for 4 representative K values. In all cases, $T = 2^{22}$ and $M = 4 \times 10^7$.

Table 1. The values of the parameters for representative K values.

$A_1 = 0.5642...$, $A_{q=1.935} = 0.3364...$				
K	B_1	B_q	α_1	α_q
0.2	—	0.015	0	1
0.6	10.7×10^{-7}	0.015	0.0380	0.9416
1	8.00×10^{-7}	0.015	0.4826	0.5078
2	1.06×10^{-7}	0.010	0.7622	0.2367
3	0.40×10^{-7}	0.010	0.8825	0.1170
10	0.52×10^{-7}	—	1	0

conditions all over the phase space and count how many of those having non-zero LLE and those having nearly zero LLE. Dividing these numbers by the total number of initial conditions, we mimic the ratio of the areas. We classify an initial condition belonging to a weakly chaotic region if its LLE is smaller than a given threshold $\lambda < \lambda_- = 5 \times 10^{-5}$. Correspondingly, an initial condition is considered to belong to a strongly chaotic region whenever $\lambda > \lambda_+ = 10^{-2}$. These limiting values λ_- and λ_+ are chosen according to what is explained in [24]: the phase-space ratio, i.e. (number of points with $\lambda < \lambda_{\text{threshold}}$)/(number of points with $\lambda > \lambda_{\text{threshold}}$) remains almost constant for $\lambda_- < \lambda_{\text{threshold}} < \lambda_+$. We call $\alpha_1 = N_{\text{ic}}(\lambda > \lambda_+)/N_{\text{ic}}$, and $\alpha_q = N_{\text{ic}}(\lambda < \lambda_-)/N_{\text{ic}}$. There remains a small amount of initial conditions with intermediate finite time LLE values ($\lambda_- \leqslant \lambda \leqslant \lambda_+$) that are not taken into account in equation (12), and that are

J. Stat. Mech. (2017) 063403

expected to be neglectable in the macroscopic limit. We have thus considered the approximated form of equation (12) as

$$P(y) \approx \alpha_q P_q(y; \mu_q, \sigma_q) + \alpha_1 P_1(y; \mu_1, \sigma_1). \tag{13}$$

The values of α_1 and α_q for some representative K values are shown in table 1. The respective values of B_1 and B_q are computed using the pdf of the system that arises from the initial conditions with positive and (nearly) zero LLE, respectively. Once B_1 and B_q values are known, we have no fitting parameter and α values are entirely determined by the intrinsic dynamics of the map. Figure 7 shows our results for some representative values of K.

6. Concluding remarks

The q-triplet (q_{ent}, q_{rel}, q_{stat}) is an important feature in the statistical description of dynamical systems that might be nonergodic and/or nonmixing, as a consequence of zero largest Lyapunov exponent (LLE). These indices define the rate of entropy production, the rate of relaxation, and the distribution of the nearly stationary states. Positive LLE leads to mixing and ergodic systems, and the strongly chaotic regime makes these three indices to collapse into $q = 1$, within the BG framework. Zero LLE characterize weak chaos and may lead to breakdown of ergodicity and nonmixing dynamics. The statistical description in many such circumstances appears to be associated with the q-entropy, where the usual exponential and Gaussian functions turn into more general forms, namely the q-exponential and the q-Gaussian ones. This scenario has been previously observed and evaluated for dissipative low-dimensional systems.

We have now considered a paradigmatic low-dimensional conservative system, namely the standard map. We have evaluated the q-triplet, and have numerically verified that the sensitivity to initial conditions index satisfies $q_{\mathrm{sen}} = q_{\mathrm{ent}}$, in both strongly and weakly chaotic regimes. Our results corroborate the expected situation, i.e. that if the entire phase space is strongly chaotic (LLE > 0), $q_{\mathrm{ent}} = q_{\mathrm{rel}} = q_{\mathrm{stat}} = 1$ and $K_{q_{\mathrm{ent}}^{\mathrm{av}}} = \lambda_{q_{\mathrm{sen}}^{\mathrm{av}}=1} \simeq 1.62 > 0$. The present results are numerically compatible with a q-generalization of a Pesin-like identity for ensemble averages, extending the results in [28] to the case of conservative maps. If the entire phase space is in a nearly weakly chaotic regime (nearly vanishing LLE), which happens for low values of K, we show that the standard map is characterized by $q_{\mathrm{ent}} = 0$, $q_{\mathrm{rel}} \simeq 1.4$, and $q_{\mathrm{stat}} \simeq 1.935$. We have also shown that $\lambda_{q_{\mathrm{sen}}^{\mathrm{av}}}$ is a property that can be characterized by the smaller alignment index (SALI), a computationally cheap tool to identify different chaotic regimes and to discriminate a variety of transient times and dynamical behaviors. The phase space for intermediate values of K exhibits regions of positive LLE and regions of zero LLE. Ensemble averages of initial conditions taken within the strongly chaotic regions behave, independently of the value of K, according to $q_{\mathrm{ent}} = q_{\mathrm{sen}} = q_{\mathrm{stat}} = 1$, and $K_{q_{\mathrm{ent}}^{\mathrm{av}}} = \lambda_{q_{\mathrm{sen}}^{\mathrm{av}}}$. In contrast, ensemble averages of initial conditions taken within the weakly chaotic regions behave according to the non degenerate q-triplet, with precisely the same values of q_{ent}, q_{sen} and q_{stat} obtained for say $K = 0.2$. This work improves what has been done in [24], as we have numerically found the proper superposition of

J. Stat. Mech. (2017) 063403

distributions for the mixed case (coexistence of strongly and weakly chaotic regimes) without any additional fitting parameter.

The q-triplet structure plays a central role on the statistical description of many nonlinear dynamical systems, and additional effort addressing other conservative and dissipative maps shall bring further tests for the robustness of this framework, and they are very welcome.

Acknowledgments

This work has been partially supported by CNPq and Faperj (Brazilian Agencies), and by TUBITAK (Turkish Agency) under the Research Project number 115F492. GR, UT and CT also acknowledge partial financial support by the John Templeton Foundation (USA).

References

[1] Tsallis C 2009 *Introduction to Nonextensive Statistical Mechanics—Approaching a Complex World* (New York: Springer)
[2] Beck C and Schlögl F 1997 *Thermodynamics of Chaotic Systems—an Introduction* (*Cambridge Nonlinear Science*) (Cambridge: Cambridge University Press)
[3] Rapisarda A and Latora V 2004 *Nonextensive Entropy—Interdisciplinary Applications* ed M Gell-Mann and C Tsallis (New York: Oxford University Press)
[4] Esquivel A and Lazarian A 2010 Tsallis statistics as a tool for studying interstellar turbulence *Astrophys. J.* **710** 125
[5] CMS Collaboration 2010 Transverse-momentum and pseudorapidity distributions of charged hadrons in pp collisions at $\sqrt{s}=7$ TeV *Phys. Rev. Lett.* **105** 022002
[6] Shao M, Yi L, Tang Z, Chen H, Li C and Xu Z 2010 Examination of the species and beam energy dependence of particle spectra using Tsallis statistics *J. Phys. G: Nucl. Part.* **37** 085104
[7] Sotolongo-Grau O, Rodríguez-Pérez D, Antoranz J C and Sotolongo-Costa O 2010 Tissue radiation response with maximum Tsallis entropy *Phys. Rev. Lett.* **105** 158105
[8] Mohanalin J, Beenamol M, Kalra P K and Kumar N 2010 A novel automatic microcalcification detection technique using Tsallis entropy and a type II fuzzy index *Comput. Math. Appl.* **60** 2426
[9] ALICE Collaboration 2010 Transverse momentum spectra of charged particles in proton–proton collisions at $\sqrt{s}=900$ GeV with ALICE at the LHC *Phys. Lett.* B **693** 53
[10] PHENIX Collaboration 2011 Measurement of neutral mesons in $p+p$ collisions at $\sqrt{s}=200$ GeV and scaling properties of hadron production *Phys. Rev.* D **83** 052004
[11] PHENIX Collaboration 2011 Nuclear modification factors of ϕ mesons in $d+\mathrm{Au}$, $\mathrm{Cu}+\mathrm{Cu}$, and $\mathrm{Au}+\mathrm{Au}$ collisions at $\sqrt{s_{NN}}=200$ GeV *Phys. Rev.* C **83** 024909
[12] ALICE Collaboration 2011 Production of pions, kaons and protons in pp collisions at $\sqrt{(}s)=900$ GeV with ALICE at the LHC *Eur. Phys. J.* C **71** 1655
[13] ATLAS Collaboration 2011 Charged-particle multiplicities in pp interactions measured with the ATLAS detector at the LHC *New J. Phys.* **13** 053033
[14] Wong C-Y and Wilk G 2013 Tsallis fits to p_{T} spectra and multiple hard scattering in pp collisions at the LHC *Phys. Rev.* D **87** 114007
[15] Marques L, Andrade E II and Deppman A 2013 Nonextensivity of hadronic systems *Phys. Rev.* D **87** 114022
[16] Bogachev M I, Kayumov A R and Bunde A 2014 Universal internucleotide statistics in full genomes: a footprint of the DNA structure and packaging? *PLoS One* **9** e112534
[17] Combe G, Richefeu V, Stasiak M and Atman A P F 2015 Experimental validation of a nonextensive scaling law in confined granular media *Phys. Rev. Lett.* **115** 238301
[18] Baldovin F and Robledo A 2002 Universal renormalization-group dynamics at the onset of chaos in logistic maps and nonextensive statistical mechanics *Phys. Rev.* E **66** 045104

[19] Ferri G L, Reynoso Savio M F and Plastino A 2010 Tsallis' q-triplet and the ozone layer *Physica* A **389** 1829

[20] Burlaga L F and Ness N F 2013 Magnetic field strength fluctuations and the q-triplet in the heliosheath: voyager 2 observations from 91.0 to 94.2 AU at latitude 30° s *Astrophys.* J **765** 35

[21] Chirikov B V 1979 A universal instability of many-dimensional oscillator systems *Phys. Rep.* **52** 263

[22] Zaslavsky G M 2005 *Hamiltonian Chaos and Fractional Dynamics* (New York: Oxford University Press)

[23] Benettin G, Galgani L, Giorgilli A and Strelcyn J-M 1980 Lyapunov characteristic exponents for smooth dynamical systems and for hamiltonian systems; a method for computing all of them *Meccanica* **15** 9

[24] Tirnakli U and Borges E P 2016 The standard map: from Boltzmann–Gibbs statistics to Tsallis statistics *Sci. Rep.* **6** 23644

[25] Baranger M, Latora V and Rapisarda A 2002 Time evolution of thermodynamic entropy for conservative and dissipative chaotic maps *Chaos Solitons Fractals* **13** 471

[26] Tsallis C, Plastino A R and Zheng W-M 1997 Power–law sensitivity to initial conditions—New entropic representation *Chaos Solitons Fractals* **8** 885

[27] Tsallis C 1994 What are the numbers that experiments provide? *Quim. Nova* **17** 468

[28] Añaños G F J and Tsallis C 2004 Ensemble averages and nonextensivity at the edge of chaos of one-dimensional maps *Phys. Rev. Lett.* **93** 020601

[29] Latora V and Baranger M 1999 Kolmogorov–Sinai entropy rate versus physical entropy *Phys. Rev. Lett.* **82** 520

[30] Latora V, Baranger M, Rapisarda A and Tsallis C 2000 The rate of entropy increase at the edge of chaos *Phys. Lett.* A **273** 97

[31] Baldovin F 2002 Mixing and approach to equilibrium in the standard map *Physica* A **305** 124

[32] Baldovin F 2004 *Nonextensive Entropy—Interdisciplinary Applications* ed M Gell-Mann and C Tsallis (New York: Oxford University Press)

[33] Tsallis C 1988 Possible generalization of Boltzmann–Gibbs statistics *J. Stat. Phys.* **52** 479

[34] Casati G, Tsallis C and Baldovin F 2005 Linear instability and statistical laws of physics *Europhys. Lett.* **72** 355

[35] Ruiz G and Tsallis C 2007 Roundoff-induced attractors and reversibility in conservative two-dimensional maps *Physica* A **386** 720

[36] Skokos C 2001 Alignment indices: a new, simple method for determining the ordered or chaotic nature of orbits *J. Phys. A: Math. Gen.* **34** 10029

[37] de Moura F A B F, Tirnakli U and Lyra M L 2000 Convergence to the critical attractor of dissipative maps: log-periodic oscillations, fractality, and nonextensivity *Phys. Rev.* E **62** 6361

[38] Borges E P, Tsallis C, Añaños G F J and de Oliveira P M C 2002 Nonequilibrium probabilistic dynamics of the logistic map at the edge of chaos *Phys. Rev. Lett.* **89** 254103

[39] Tirnakli U, Beck C and Tsallis C 2007 Central limit behavior of deterministic dynamical systems *Phys. Rev.* E **75** 040106

[40] Tirnakli U, Tsallis C and Beck C 2009 Closer look at time averages of the logistic map at the edge of chaos *Phys. Rev.* E **79** 056209

[41] Ruiz G, Bountis T and Tsallis C 2012 Time-evolving statistics of chaotic orbits of conservative maps in the context of the central limit theorem *Int. J. Bifurcation Chaos* **22** 1250208

[42] Prato D and Tsallis C 1999 Nonextensive foundation of Lévy distributions *Phys. Rev.* E **60** 2398

J. Stat. Mech. (2017) 063403